Energy Transmission via a Cascade of Coupled Coils

R. M. Howard & I. M. Howard
Curtin University of Technology
GPO Box U1987, Perth, Western Australia, 6845
r.howard@exchange.curtin.edu.au

Abstract--**The modelling of a *N* stage cascade of coupled coils is detailed for the general homogenous case and the specific non-homogenous case associated with energy coupling in joined pipe structures. Consistent with the practical situation, models are developed assuming the coils have different radii and have a lateral offset. A resonant structure, which facilitates energy transmission, is proposed. It is shown that the ability to transfer energy is relatively insensitive to frequency, within a few percent of the resonant frequency, to component tolerance and to load resistance. However, it is shown to be critically dependent on the level of mutual coupling between the two coils. It is practical for energy transmission, at greater than a 10*mW *level, over 8 stages consistent with a distance of 80*m**.

Keywords--inductive power transfer; coupled coils; resonance.

I. INTRODUCTION

There are many applications where transfer of energy, without the use of an end to end electrical conductor, is required or is desirable, including passive RFID, e.g. [1], bionic systems, e.g. [2], and inductive power transfer systems, e.g. [3]. Normally, single stage coupling is used, e.g. [1], [2] and [3]. However, there exists situations, including powering remotely located sensors, for example, at a distance down an oil/gas well, where energy transfer over N widely separated coupled coil stages is required. For such situations frequencies below RF are required; normally for low power applications RF frequencies are used and short distances are involved, e.g. [2].

In this paper the modelling of a N stage cascade of coupled coils is detailed for both the general homogenous case and the specific non-homogenous case associated with energy coupling in joined pipe structures. Models are developed, consistent with the practical situation, where the coils have different radii and a lateral offset. A resonant structure, which facilitates energy transmission is proposed. Several factors affecting energy transmission are detailed. The approach can readily be adapted for other coupled coil structures. Section II details appropriate modelling of two coupled coils and in Section III the modelling of a cascade of such coils is considered. Results are discussed in section IV.

II. MODELLING

Consider the situation of energy transmission over a single stage of a N stage energy transmission system where one stage is characterized, consistent with the situation of pipe casing, by a length of conducting wire leading to two coupled coils. The first issue is the modelling of the coupled coils and, in general, they have different radii, and a lateral offset h, as illustrated in Fig. 1. To ensure generality, models are established, first, for the case of a linear homogenous medium with permeability μ and, second, consistent with a pipe structure, for a non-homogenous medium.

A. Inductance: Homogenous Case

Consider the case of two loosely coupled coils illustrated in Fig. 1. The assumption is made, consistent with the situation of cylindrical structures, that the radii ρ_1 and ρ_2 are large relative to the wire radius, denoted a. It then follows, with a low to moderate number of turns, that the approximation of the turns being co-located, as illustrated in Fig. 1, is reasonable. The current I_1 in coil 1 creates a magnetic flux density $\underset{\sim}{B}_1$ and, hence, a flux through the second coil according to

$$\Phi_{21} = N_2 \int_{S_2} \underset{\sim}{B}_1 \bullet d\underset{\sim}{S}_2 . \qquad (1)$$

By definition of mutual inductance $L_{21} = \Phi_{21}/I_1$, and as outlined in Appendix 1, it follows that

$$L_{21} = \frac{\mu N_1 N_2 \rho_o}{4\pi} \cdot k(\Delta, h/\rho_o) . \qquad (2)$$

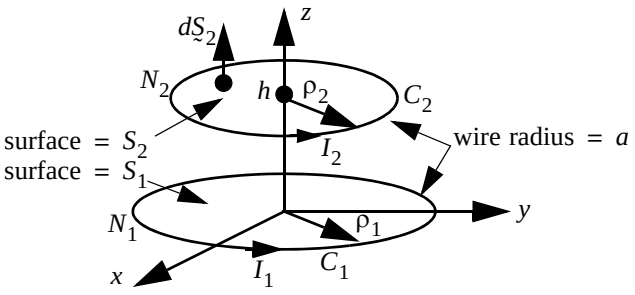

Figure 1. Coupled coil structure. The first coil, with N_1 turns and radius ρ_1 is defined by the curve C_1. The second coil, with N_2 turns and radius ρ_2 is defined by the curve C_2.

where $\rho_1 = \rho_o(1+\Delta/2)$, $\rho_2 = \rho_o(1-\Delta/2)$,

$$\rho_o = (\rho_1+\rho_2)/2, \quad \Delta = 2(\rho_1-\rho_2)/(\rho_1+\rho_2), \tag{3}$$

$$k(\Delta,\gamma) = \int_0^{2\pi}\int_0^{2\pi} \frac{\sqrt{1-\Delta^2/4}\ \cos(\theta_1-\theta_2)d\theta_1 d\theta_2}{\sqrt{2}\sqrt{\dfrac{1+\Delta^2/4+\gamma^2/2}{1-\Delta^2/4}-\cos(\theta_1-\theta_2)}}. \tag{4}$$

Similarly $L_{12} = \Phi_{12}/I_2$ and it follows that $L_{12} = L_{21}$. The procedure to establish L_{12} and L_{21} is general and consistent with the approach that underpins Neumann's formula, e.g. [4]. The function $k(\Delta,\gamma)$ is shown in Fig. 2.

To establish the self inductance of the two coils the following approach is used as considering an ideal coil with zero radius results in the self inductance being indeterminate [5]: First, the wire radius a needs to be considered and the model shown in Fig. 3 for the first coil is appropriate. Second, external to the wire it can be shown, using Ampere's law, that the magnetic flux density is the same as that produced by an ideal coil with zero dimensions and centered at the center of the practical coil. Third, the flux through the interior surface of the coil is

$$\Phi_1 = N_1 \int_{S_{\text{Int}}} \underset{\sim}{B}_1 \bullet d\underset{\sim}{S}_{\text{Int}}. \tag{5}$$

This flux is the same as the mutual flux through an ideal second coil, which is co-centric and co-planer with the first coil, with N_1 turns and with radius $\rho_1 - a$. Thus, with the definition $L_1 = \Phi_1/I_1$ it follows from (2) that

$$L_1 = L_{21}\big|_{N_2 = N_1,\, h = 0,\, \rho_2 = \rho_1 - a} \tag{6}$$

and, hence

$$L_1 = \frac{\mu N_1^2}{4\pi}\left(\rho_1 - \frac{a}{2}\right) k\left(\frac{a}{\rho_1 - a/2}, 0\right). \tag{7}$$

Similarly

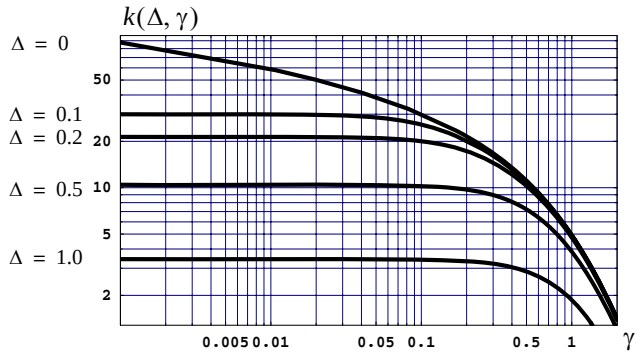

Figure 2. Graph of $k(\Delta,\gamma)$.

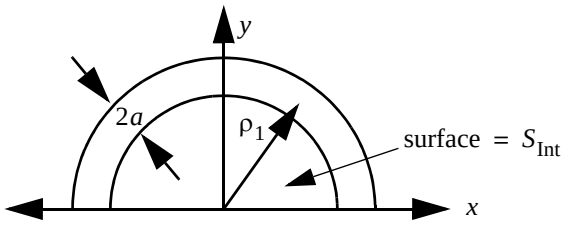

Figure 3. Model for determining the self inductance of the first coil with wire radius a. A top view is shown. The surface S_{Int} is defined as the interior of the loop defined by the wire.

$$L_2 = \frac{\mu N_2^2}{4\pi}\left(\rho_2 - \frac{a}{2}\right) k\left(\frac{a}{\rho_2 - a/2}, 0\right). \tag{8}$$

B. Inductance: Non-homogenous Case

Consider the case of coupling between two coils when they are embedded in a cylindrical structure, as illustrated in Fig. 4, with inner radius ρ_I, and permeability μ which is significantly higher than μ_o. This structure is consistent with two coils embedded in two different lengths of pipe which are then mechanically connected together via a threaded joint.

An approximate method of establishing the inductances associated with such a structure is to first, establish the flux flowing through either coil assuming a homogenous medium with permeability μ. Second, establish the flux flowing through an imaginary coil of radius ρ_I, and with surface area S_I, assuming the same homogenous medium. Third, the actual flux flowing through the coil is then, approximately, the difference of the two fluxes. Thus:

$$\Phi_{21} \approx N_2\left[\int_{S_2} \underset{\sim}{B}_1 \bullet d\underset{\sim}{S}_2 - \int_{S_I} \underset{\sim}{B}_1 \bullet d\underset{\sim}{S}_I\right]. \tag{9}$$

Assuming $\rho_1 \approx \rho_2 = \rho$ it then follows that

$$L_{21} = L_{12} = \frac{\mu N_1 N_2}{4\pi} \cdot \left[\rho k\left(0, \frac{h}{\rho}\right) - \rho_{oI} k\left(\Delta_I, \frac{h}{\rho_{oI}}\right)\right] \tag{10}$$

where

$$\rho_{oI} = (\rho+\rho_I)/2, \quad \Delta_I = 2(\rho-\rho_I)/(\rho+\rho_I). \tag{11}$$

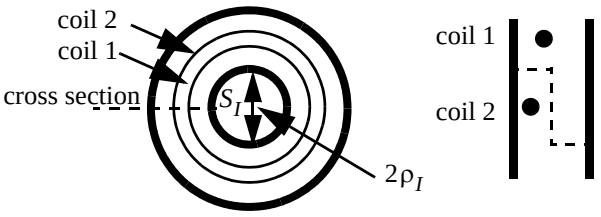

Figure 4. Left: Top view of coils when embedded in a cylindrical structure. Right: Front view of cross section of cylindrical structure. The dotted line indicates the threaded joint between the two cylindrical structures.

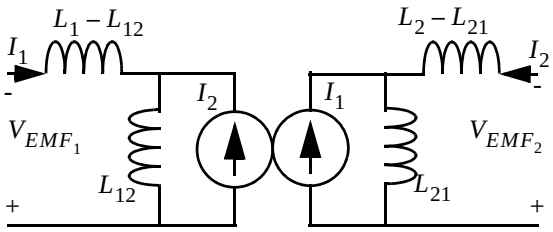

Figure 6. Equivalent circuit model for coupled coils.

Similarly, with $N_1 = N_2 = N$:

$$L_1 = L_2 = \frac{\mu N^2}{4\pi}\left[\left(\rho - \frac{a}{2}\right)k\left(\frac{a}{\rho - a/2}, 0\right) - \rho_{oI}k(\Delta_I, 0)\right]. \quad \textbf{(12)}$$

The results are approximate as they assume $\mu \gg \mu_o$, ignore the effect of the boundary conditions between the high and low permeability regions, and assume $\underset{\sim}{B} = \mu \underset{\sim}{H}$.

C. Equivalent Model of Coupled Coils

Consider the coupled coil model illustrated in Fig. 5. The electromotive force generated in the loops, according to Faraday's law, are

$$V_{EMF_1} = -\frac{d}{dt}(\Phi_1 + \Phi_{12}), \quad V_{EMF_2} = -\frac{d}{dt}(\Phi_2 + \Phi_{21}) \quad \textbf{(13)}$$

and from the definitions of inductance and mutual inductance, e.g. $L_1 = \Phi_1 / I_1$ and $L_{12} = \Phi_{12} / I_2$, it then follows that

$$V_{EMF_1} = -L_1\frac{dI_1}{dt} - L_{12}\frac{dI_2}{dt}, \quad V_{EMF_2} = -L_2\frac{dI_2}{dt} - L_{21}\frac{dI_1}{dt}. \quad \textbf{(14)}$$

The equivalent model shown in Fig. 6 then follows. For the symmetrical case of $L_{12} = L_{21}$ the simplified model shown in Fig. 7 results, where resistances R_1 and R_2 have been added to account, respectively, for the resistance of the first and second coils and the associated resistance of the conducting wires leading to and from the coils [6].

III. CASCADE OF COUPLED COILS

Consider the case of a cascade of N coils, where each coil has the equivalent circuit illustrated in Fig. 7, and a capacitor,

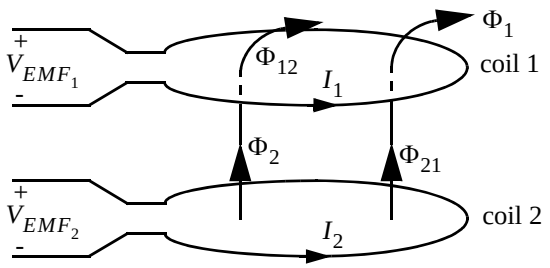

Figure 5. Definition and illustration of electromotive force generated in coupled coils.

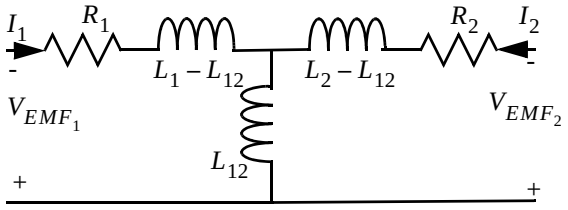

Figure 7. Simplified circuit model for the symmetrical case defined by $L_{12} = L_{21}$.

C_1, has been added to the input of each stage such that the kth loop is as shown in Fig. 8. The capacitor C_1 is chosen such that a specified resonant frequency, f_o, is defined according to

$$f_o = 1/2\pi\sqrt{(L_1 + L_2)C_1}. \quad \textbf{(15)}$$

The structure, and the resonant frequency, have been chosen such that at resonance the circuit has the ideal model shown in Fig. 9. This is not the usual resonant condition used for a single coupled coil, e.g. [2], but is the condition that facilitates energy transmission over N stages for $N \geq 2$. Energy transmission is facilitated when the magnitude of the impedance of L_{12} is much greater than $R_1 + R_2$. Other resonant structures are possible but, in general, they lead, assuming ideal component values, to an extremely narrow frequency range of high gain and significant attenuation away from the resonant frequency. For practical component values, and for a moderate number of stages, such resonant conditions lead, in general, to significant attenuation.

Consistent with Fig. 8, the mesh equation for the kth loop is

$$-I_{k-1}sL_{12} + I_k\left[R_1 + R_2 + s(L_1 + L_2) + \frac{1}{sC_1}\right] - I_{k+1}sL_{12} = 0, \qquad k \in \{1, \ldots, N-1\}. \quad \textbf{(16)}$$

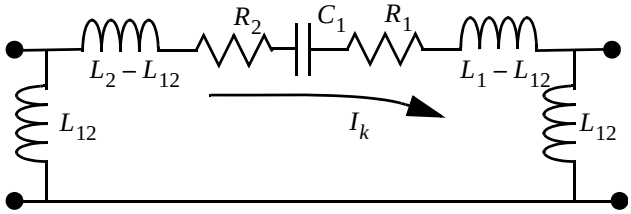

Figure 8. Circuit for kth loop of a N stage cascade of coupled coils.

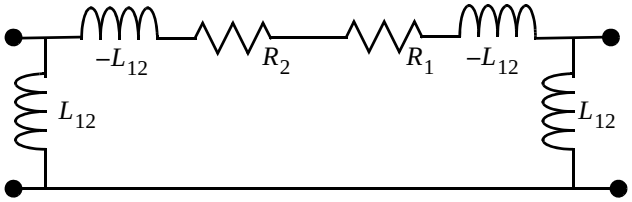

Figure 9. Model for kth loop at resonance.

The zeroth order, and the Nth loop equations are:

$$-V_S + I_0\left[R_S + R_1 + s(L_1 + L_2) + \frac{1}{sC_1}\right] - I_1 sL_{12} = 0$$
$$-I_{N-1} sL_{12} + I_N\left[R_2 + R_L + s(L_1 + L_2) + \frac{1}{sC_1}\right] = 0 \quad \textbf{(17)}$$

where R_S is the source resistance, R_L is the load resistance, and impedances $sL_2 + 1/sC_1$ and $sL_1 + 1/sC_1$ have been added, respectively, to the input of the first stage and to the load. The load voltage can be determined according to $V_L = I_N R_L$. Solving these $N+1$ equations allows the transfer function V_L/V_S and the power transferred to the load, i.e. $P_L = V_L^2/R_L$, to be determined.

IV. RESULTS

Results are detailed for the homogenous case, e.g. free space case, and for the non-homogenous case. The results are presented for the case of coils with a diameter of $0.1m$ - consistent with tubing used for oil/gas pipes. Copper wire with a radius of $a = 5x10^{-3}m$ is assumed and a resistance of 0.5Ω is consistent with a pipe length of $10m$ and a total wire length of $20m$ plus coil length. Source and load resistances, respectively, of 1Ω and 100Ω are assumed. For both cases a resonant frequency has been chosen which is low enough such that the quasi-static assumption underpinning magnetostatic principles is valid, and capacitive effects associated with the inductors is small. Also, the resonant frequency has been chosen high enough to ensure a moderate inductance impedance level relative to the conductor resistance level, which, in turn, ensures good energy transmission.

A. Homogenous Case

Consider the homogenous case where $\mu = \mu_o$ and with parameters $N_1 = N_2 = 10$, $\rho_o = 0.05$, $\Delta = 0.02$, a moderate offset of $h/\rho_o = 0.5$, whereupon the following approximate values are valid:

$$L_1 \approx L_2 \approx 29\mu H, \qquad L_{12} = L_{21} \approx 5.5\mu H. \quad \textbf{(18)}$$

A resonant frequency of $500kHz$ provides good performance and, according to (15), $C_1 = 1.75nF$. Using these parameters, and solving the $N+1$ equations defined by (16) and (17), the transfer function is illustrated in Fig. 10 and Fig. 11 for the cases, respectively, of ideal component values and component values with a 5% tolerance.

B. Non-Homogenous Case

Consider the case of a steel based pipe with inside and outside radii, respectively of $0.057m$ and $0.043m$. With

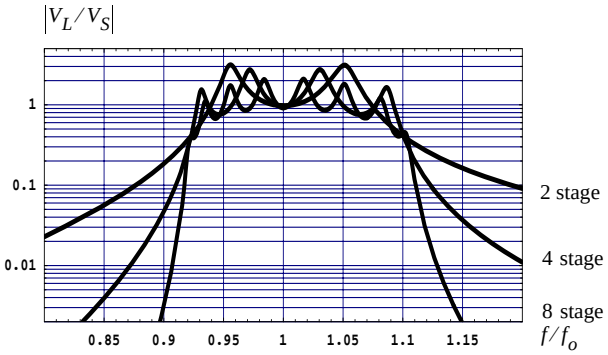

Figure 10. Transfer function for the homogenous case, a resonant frequency of 500 kHz and ideal components with zero tolerance.

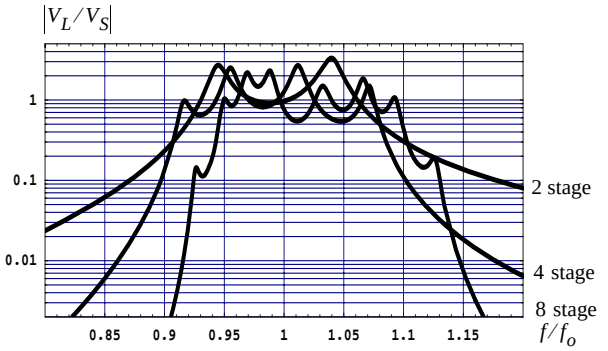

Figure 11. Transfer function for the homogenous case, a resonant frequency of 500 *kHz* and component tolerances of 5% have been assumed.

$\mu = 2600\mu_o$, $\rho_1 \approx \rho_2 = 0.05$, $\Delta_I = 0.007m$, $N_1 = 2$, $N_2 = 2$, and $h/\rho_o = 0.5$ the following approximate values are valid:

$$L_1 \approx L_2 \approx 1840\mu H, \qquad L_{12} = L_{21} \approx 97\mu H. \quad \textbf{(19)}$$

Consistent with the assumptions made, a resonant frequency of $50kHz$ provides good performance and, according to (15), $C_1 = 2.75nF$. The magnitude of the transfer function is plotted in Fig. 12 assuming 5% component tolerance. With higher resistance values of $R_1 = R_2 = 2.5\Omega$, to account for additional losses, the performance is impacted by about a factor of two.

C. Discussion

The following observations can be made for both the homogenous and non-homogenous cases: First, the transfer function is relatively insensitive, when compared to a standard resonant circuit, to component tolerances for frequencies within a few percent of the resonant frequency. This arises from the resonant structure used. Second, the frequency range over which there is moderate gain/moderate attenuation, is broad at a few percent of the resonant frequency. Third, the transfer function is dependent, consistent with Fig. 9, on the mutual inductance and, hence, on the ratio L_{12}/L_1. This is clearly evident from the results for the homogenous and non-

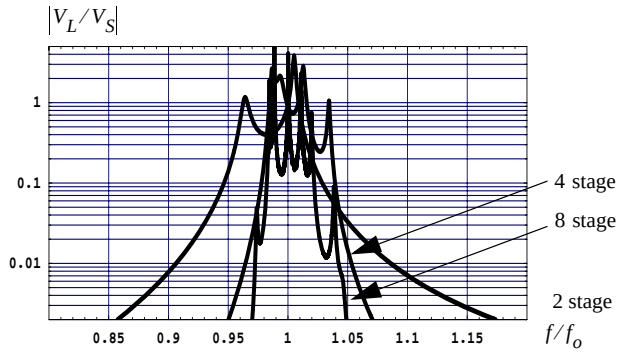

Figure 12. Transfer function for the homogenous case, a resonant frequency of 50 kHz and component tolerances of 5% have been assumed.

homogenous cases. Significantly improved results can be obtained for the non-homogenous case when the ratio L_{12}/L_1 is increased. This ratio depends, consistent with Fig. 2, on the lateral offset as given by h/ρ_o. For the homogenous case a low lateral offset of $h/\rho_o = 0.1$ yields little attenuation, at the resonant frequency, after 15 stages. In contrast, a high lateral offset of $h/\rho_o = 1.0$ results in an attenuation level of 0.1 after 10 stages. Fourth, the performance is relatively insensitive to load resistance for resistances greater than about 20Ω. Hence, with unity gain after 8 stages, a $10V$ signal source and a load resistance of 100Ω, the average power delivered to the load is $1W$. For the case, due to component tolerance, where the attenuation is 0.1, the transmitted power is $10mW$. Finally, the attenuation increases dramatically after a certain number of stages. For the homogenous case the attenuation, at the resonant frequency, is approximately 0.5 for 12 stages but falls to 0.05 for 13 stages.

V. CONCLUSION

The modelling of a N stage cascade of coupled coils has been detailed for both the general homogenous case and the specific non-homogenous case associated with energy coupling in joined pipe structures. Consistent with the practical situation, models were developed assuming the coils have different radii and a lateral offset. A resonant structure, which facilitates energy transmission, was proposed. It is shown that the ability to transfer energy is relatively insensitive to frequency, within a few percent of the resonant frequency, to component tolerance and to load resistances above 20Ω. However, it was shown to be critically dependent on the level of mutual coupling between the two coils. It is practical to achieve energy transmission, at greater than the $10mW$ level, over 8 stages consistent with a distance of 80m. Further optimization is possible, e.g. [7], and the next stage is to accurately model the non-linear relationship between $\underset{\sim}{B}$ and $\underset{\sim}{H}$ for the non-homogenous case.

APPENDIX 1: MUTUAL INDUCTANCE

The evaluation of flux, as specified by (1) is facilitated by using the magnetic vector potential $\underset{\sim}{A}$, the relationship $\underset{\sim}{B} = \nabla \times \underset{\sim}{A}$ and Stoke's theorem, to yield

$$\Phi_{21} = N_2 \int_{C_2} \underset{\sim}{A}_1 \bullet d\underset{\sim}{r}_2 \tag{20}$$

where

$$C_2 = \{\underset{\sim}{r}_2 : \underset{\sim}{r}_2(\theta_2) = \rho_2\cos(\theta_2)\underset{\sim}{i} + \rho_2\sin(\theta_2)\underset{\sim}{j} + h\underset{\sim}{k}, \quad \theta_2 \in (0, 2\pi)\}. \tag{21}$$

The elemental path length $d\underset{\sim}{r}_2$ along C_2 is given by

$$d\underset{\sim}{r}_2 = [-\rho_2\sin(\theta_2)\underset{\sim}{i} + \rho_2\cos(\theta_2)\underset{\sim}{j}]d\theta_2 \tag{22}$$

and along the curve C_2 the magnetic vector potential due to the current I_1, flowing in the curve C_1, is

$$\underset{\sim}{A}_1(\underset{\sim}{r}_2) = \frac{N_1\mu I_1}{4\pi}\int_{C_1}\frac{d\underset{\sim}{r}_1}{|\underset{\sim}{r}_2 - \underset{\sim}{r}_1|}. \tag{23}$$

Here

$$C_1 = \{\underset{\sim}{r}_1 : \underset{\sim}{r}_1(\theta_1) = \rho_1\cos(\theta_1)\underset{\sim}{i} + \rho_1\sin(\theta_1)\underset{\sim}{j} \quad \theta_1 \in (0, 2\pi)\} \tag{24}$$

and the elemental path length $d\underset{\sim}{r}_1$ along C_1 is given by

$$d\underset{\sim}{r}_1 = [-\rho_1\sin(\theta_1)\underset{\sim}{i} + \rho_1\cos(\theta_1)\underset{\sim}{j}]d\theta_1. \tag{25}$$

Evaluation of $|\underset{\sim}{r}_2 - \underset{\sim}{r}_1|$ and substitution of (23) into (20) yields (2) and the definition of $k(\Lambda, h/\rho_o)$ as given by (4).

REFERENCES

[1] V. Chawla & Dong Sam Ha, 'An overview of passive RFID', IEEE Communications Magazine, vol. 45, Sept. 2007, pp 11-17.

[2] M. W. Baker & R. Sarpeshkar, 'Feedback analysis and design of RF power links for low-power bionic systems', IEEE Transactions on Biomedical Circuits and Systems, vol. 1, 2007, pp. 28-38.

[3] J. T. Boys, G. A. Covic & A. W. Green, 'Stability and control of inductively coupled power transfer systems', IEE Proceedings: Electric Power Applications, vol. 147, 2000, pp. 37-43.

[4] S. Ramo, J. R. Whinnery & T. Van Duzer, Fields and Waves in Communication Electronics, 2nd ed., Wiley, 1984, p. 189.

[5] R. Bansal (Ed.), Handbook of Engineering Electromagnetics, Marcel Dekker, 2004, p. 154.

[6] W. H. Hayt & J. E. Kemmerly, 'Engineering Circuit Analysis', McGraw Hill, 1978, p. 503.

[7] C. M. Zierhofer & E. S. Hochmair, 'Geometric approach for coupling enhancement of magnetically coupled coils', IEEE Transactions on Biomedical Engineering, vol. 43, pp. 708-714, 1996.